

Spin Currents in Rashba Altermagnets: From Equilibrium to Nonlinear Regimes

¹Priyadarshini Kapri*

Department of Mathematics and Physics, North Carolina Central University, Durham, NC-27707, USA

(Dated: June 18, 2025)

We investigate equilibrium (background), linear, and nonlinear spin currents in two-dimensional Rashba spin-orbit coupled altermagnet systems, using a modified spin current operator that includes anomalous velocity from non-zero Berry curvature. The background spin current, stemming from spin-orbit coupling and modulated by the altermagnet term (t_j), exhibits in-plane polarization, increases linearly with Fermi energy (ϵ_F), and is enhanced by both the altermagnet (t_j) and the Rashba parameter (λ). Linear spin current is always transverse with out-of-plane polarization and can be viewed as Spin Hall current, primarily driven by band velocity, with t_j enabling a band-induced contribution (previously absent in simple Rashba systems ($t_j = 0$)). This highlights altermagnet system as a promising source of spin Hall current generation. For linear spin Hall current, its band contribution's magnitude increases linearly with ϵ_F , while the magnitude of anomalous component saturates at higher ϵ_F . Further, the magnitude of spin Hall current is enhanced by t_j but reduced by λ . Nonlinear spin currents feature both longitudinal and transverse components with in-plane polarization. Both the nonlinear longitudinal spin current from band velocity and the nonlinear transverse spin current from anomalous velocity initially decrease with ϵ_F before saturating at higher ϵ_F . Importantly, t_j reduces these currents while λ enhances them. Meanwhile, the nonlinear transverse current from band velocity increases and then saturates with ϵ_F , enhanced by λ and showing non-monotonic variation with t_j . These findings highlight the tunability of spin current behavior through Rashba and altermagnet parameters, offering insights for spintronic applications.

I. INTRODUCTION

A recent breakthrough in magnetism involves the discovery of a class of antiferromagnetic materials known as altermagnets. These materials feature strongly spin-polarized itinerant electrons but lack overall magnetization. Altermagnets have a unique spin-split band structure that arises from mechanisms other than relativistic effects like spin-orbit coupling. Additionally, they do not exhibit invariance under the combined operations of parity and time-reversal [1]. These properties enable the intrinsic generation of spin currents, which are crucial for advancing spintronic technologies. The spin-splitting observed in altermagnets can reach substantial magnitudes, up to the scale of an electron volt. Due to their intriguing physical characteristics and potential applications in spintronics, altermagnets have garnered significant attention within the condensed matter community. The duality of real-space antiferromagnetism and reciprocal-space anisotropic spin polarization, akin to ferromagnetism, allows altermagnetic materials to exhibit many novel physical effects. These include giant magnetoresistance (GMR) effect [2], piezomagnetic effect [3], spin-splitting torque [4–7], tunneling magnetoresistance (TMR) effect [2, 8], time-reversal odd anomalous effect [9–14], higher-order topological states [15], altermagnetic ferroelectricity [16], nontrivial superconductivity [17, 18], quantum anomalous Hall effect [19] and strong spin-orbit coupling effects in light element altermagnetic materials [20]. Additionally, predicted altermagnetic materials span metals, semimetals, and insulators, ensuring the po-

tential realization of these novel physical effects in experiments [21–24].

Thus far, a diverse array of materials has been categorized as altermagnets, including RuO_2 [25], MnTe [26, 27], MnF_2 [28] and others. However, the majority of documented altermagnets are three-dimensional (3D), with only limited reports on two-dimensional (2D) variants. Additionally, theoretical predictions have identified some 2D altermagnets, such as $\text{V}_2\text{Te}_2\text{O}$ [29] and RuF_4 [30]. Studies have demonstrated that monolayer $\text{MnP}(\text{S}, \text{Se})_3$ can transition from antiferromagnetism to altermagnetism through the application of an electric field or by adopting a Janus structure, which disrupts inversion symmetry between sublattices [31].

The generation and control of spin currents lie at the heart of spintronics, a field that aims to exploit both the spin and charge attributes of carriers to control the properties of materials and devices [32–35]. Traditionally, spin current generation has relied on spin injection or pumping from neighboring ferromagnets [36–41], optical injection [42, 43] methods that rely on optical selection rules. Another significant approach uses heavy metals that exhibit strong spin-orbit coupling (SOC). Here, it is worth noting that Rashba spin-orbit coupling (RSOC) [44, 45] (a specific form of SOC arising from the absence of surface inversion symmetry in electron confinement within quantum wells or heterostructures) is of notable significance in the advancing field of spintronics, enabling the development of novel devices with the ability to adjust the RSOC strength through external gate voltages or alternative approaches [46, 47]. While these approaches have significantly advanced the field, they face inherent limitations. Ferromagnets introduce problematic stray magnetic fields that hinder device scaling and integration density, while conventional heavy metals often de-

* pkapri@ncsu.edu

mand high power consumption and are restricted by the need for strong SOC, thereby limiting material design flexibility. These challenges underscore a critical need for alternative materials and mechanisms for robust and efficient spin current generation.

As discussed earlier, altermagnets possess a collinear antiferromagnetic-like ordering with zero net magnetization, yet they exhibit momentum-dependent spin splitting in their electronic band structure, even in the absence of SOC. These properties make altermagnets promising platforms for efficient intrinsic spin current generation. Moreover, the absence of stray magnetic fields and the potential for ultrafast spin dynamics make altermagnets highly suited for dense integration in next-generation spintronic memory and logic devices. Thus, understanding the spin transport properties in altermagnet systems is fundamentally important and strategically valuable for advancing scalable, energy-efficient technologies.

Inspired by the preceding discussion, we consider a 2D system that integrates Rashba spin-orbit coupling with altermagnetism [48], given their significant individual contributions to spin current generation. In this model, the Rashba term breaks inversion symmetry, while the altermagnet term breaks the combined parity (P) and time-reversal (T) symmetry (PT symmetry). The discrete symmetries of the Hamiltonian significantly influence the behavior of spin currents. The presence of inversion and time reversal symmetry leads to the elimination of even and odd-order contributions of the electric field to the spin current, respectively [49]. As symmetries play a crucial role in determining the fate of spin currents, we focus on how these broken symmetries in our system contribute to the generation of different order spin currents. With the symmetry analysis one can justify the existence of a finite spin current in noncentrosymmetric systems (absence of inversion symmetry) under thermodynamic equilibrium conditions (i.e. in absence of an electric field), referred to as background equilibrium spin current [50, 51]. This spin current, while present, cannot transport or accumulate electron spins. The spin-orbit interaction acts as the driving force for spins, resulting in a pure persistent spin current. A significant amount of research has been dedicated to the study of persistent spin current [52–57]. Among various possibilities, the linear spin Hall current has emerged as a prominent technique for generating and manipulating spin currents [58, 59]. Moreover, there has been a growing interest in producing nonlinear spin currents [49, 60–62]. Nonlinear spin current can emerge in various scenarios, such as in a 2D crystal with Fermi surface anisotropy [60] or in a non-centrosymmetric spin-orbit coupled system [49, 61], with a simple application of an electric field \mathbf{E} . Our investigation therefore aims to explore the equilibrium, linear, and nonlinear spin currents within this framework, particularly emphasizing how the interplay between Rashba and altermagnet parameters influences spin current behavior as a function of Fermi energy.

This paper is structured as follows: In Sec. (IIA) and Sec. (IIB), we discuss the formalism of spin current for a generic two-band system. Section (IIC) encompasses the fundamental details regarding the 2D altermagnet Rashba system. Section (III) includes associated findings on different order spin currents. Lastly, in Sec. (IV), we offer concluding remarks and summarize our main results.

II. THEORY

This section outlines a general formalism for spin currents of different orders in a two-band system subjected to an external electric field. We begin by exploring how the modified Fermi-Dirac distribution function under an external electric field allows us to define various orders of spin currents. Subsequently, we offer an overview of a 2D Rashba-coupled altermagnet system.

A. Approximation in the carrier distribution function

For the correction to the particle distribution function, our study adopts the approach of Ref. [61], where the derivation considers the local change in the equilibrium distribution function caused by the applied field.

When a system is subjected to a spatially uniform electric field \mathbf{E} , the electron energy is changed to $\epsilon'(\mathbf{r}, \mathbf{k}) = \epsilon(\mathbf{k}) + e\mathbf{E} \cdot \mathbf{r}$, with \mathbf{r} being the spatial coordinate. Since the change in electron energy is very weak as compared to the Fermi energy ϵ_F , the Fermi-Dirac distribution function $f(\mathbf{r}, \mathbf{k}) = (1 + e^{\beta[\epsilon'(\mathbf{r}, \mathbf{k}) - \epsilon_F]})^{-1}$ with $\beta = 1/(k_B T)$ can be expanded in a series of terms proportional to powers of \mathbf{E} . Here, it is to be noted that the linear term is constrained to replicate the solution of the Boltzmann transport equation (BTE). Hence, the spatial coordinate must be written in the form $\mathbf{r} = \mathbf{v}_b \tau$ with τ being the relaxation time and \mathbf{v}_b being the band velocity. With this consideration, the modified distribution function can be expressed as [61]

$$f(\epsilon, \mathbf{E}, \tau) = \sum_n f_n = \sum_n \frac{[e\tau \mathbf{E} \cdot \mathbf{v}_b]^n}{n!} \frac{\partial^n}{\partial \epsilon^n} [f_0(\epsilon)], \quad (1)$$

where $n = 0, 1, 2, \dots$ and $f_0(\epsilon) = (1 + e^{\beta[\epsilon(\mathbf{k}) - \epsilon_F]})^{-1}$ being the equilibrium distribution function in absence of the electric field. The term $f_n (\sim E_\eta^n, \eta: \text{direction of electric field})$ denotes the n -th order deviation from the equilibrium distribution function $f_0(\epsilon)$ due to the external electric field.

B. Redefinition of spin current

In the presence of an external electric field \mathbf{E} , a system with non-zero Berry curvature ($\mathbf{\Omega}$) causes charge carriers

to acquire an additional velocity transverse to the direction of the electric field. This additional velocity is commonly known as anomalous velocity. The velocity operator, including the anomalous term— $\hat{v}_i = \hat{v}_{b,i} + \hat{v}_{a,i}$, where $\hat{v}_{b,i} = \frac{1}{\hbar} \frac{\partial H(\mathbf{k})}{\partial k_i}$ is the band velocity operator (H : Hamiltonian, \mathbf{k} : wavevector), and $v_{a,i} = -(e/\hbar)\epsilon_{ijk}E_j\Omega_k$ (Ω_k : Berry curvature in k direction) represents the anomalous velocity in i direction—is well established and widely employed in the literature [63–65], with the anomalous component being central to the anomalous Hall effect (AHE). In the conventional definition of the spin current operator, only the band velocity contribution is considered, while the contribution from the anomalous velocity is completely neglected. The conventional definition of the spin current operator is given by: $\hat{v}_{b,ij} = (\hat{v}_{b,i}\sigma_j + \sigma_j\hat{v}_{b,i})/2$, where the first index i denotes the direction of propagation, the second index j specifies the spin orientation of the charge carrier and σ represents the Pauli's Matrices. With inclusion of anomalous velocity, the redefined spin current operator is given by [62]

$$\hat{v}_{ij} = \hat{v}_{b,ij} + \hat{v}_{a,ij}, \quad (2)$$

where $\hat{v}_{a,ij} = v_{a,i}\sigma_j$. With the above defined spin current operator, the total spin current can be expressed as

$$\mathcal{J}_{ij}^{(n)} = \frac{\hbar}{2} \sum_{n,s} \int \frac{d^D \mathbf{k}}{(2\pi)^D} \langle s, \mathbf{k} | \hat{v}_{ij} | s, \mathbf{k} \rangle f_n, \quad (3)$$

where D denotes the spatial dimension of the system under consideration and $s = \pm$ denotes the band indices. Thus, the spin current of the n -th order arising from the band velocity is given by

$$\mathcal{J}_{b,ij}^{(n)} = \frac{\hbar}{2} \sum_s \int \frac{d^D \mathbf{k}}{(2\pi)^D} \langle s, \mathbf{k} | \hat{v}_{b,ij} | s, \mathbf{k} \rangle f_n. \quad (4)$$

It is important to note that for $n = 0$, the zeroth-order spin current ($\mathcal{J}_{xy}^{(0)} = \mathcal{J}_{b,xy}^{(0)}$), also known as the background spin current, originates exclusively from the band velocity, while the lowest-order contribution from the anomalous velocity appears at first order, since the anomalous velocity $\mathbf{v}_a \propto \mathbf{E}$. Consequently, the $(n+1)$ -th order spin current originating from the anomalous velocity can be expressed as

$$\mathcal{J}_{a,ij}^{(n+1)} = \frac{\hbar}{2} \sum_s \int \frac{d^D \mathbf{k}}{(2\pi)^D} \langle s, \mathbf{k} | \hat{v}_{a,ij} | s, \mathbf{k} \rangle f_n. \quad (5)$$

Finally, the total spin current of order n can be calculated as $\mathcal{J}_{ij}^{(n)} = \mathcal{J}_{b,ij}^{(n)} + \mathcal{J}_{a,ij}^{(n)}$.

C. Rashba coupled altermagnet system

The Hamiltonian for a two dimensional Rashba coupled altermagnet system is given by [48]

$$H = t_0 \sigma_0 k^2 + 2t_j \sigma_z k_x k_y + \lambda (\sigma_y k_x - \sigma_x k_y), \quad (6)$$

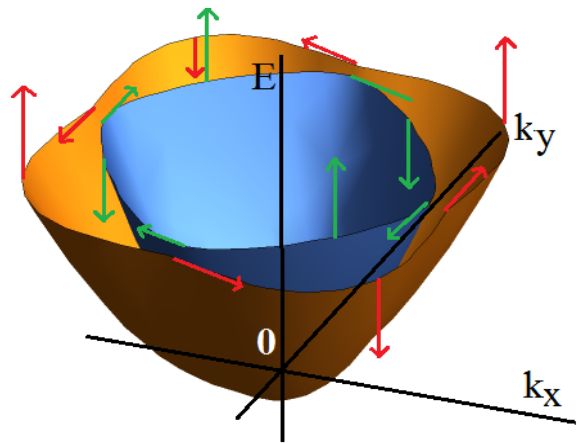


FIG. 1. The two level energy spectrum of the Hamiltonian in Eq. (6). The two types of arrows show the spin orientation about a constant energy contour.

where $\mathbf{k} = \{k \cos \phi, k \sin \phi\}$ is the electron's wave vector, t_0 is kinetic nearest neighbor hopping, t_j is parameter that characterizes the altermagnetism strength, λ is the strength of Rashba spin-orbit coupling, $\sigma = (\sigma_x, \sigma_y, \sigma_z)$ represents the usual Pauli's matrices and σ_0 is the 2×2 identity matrix. The two level energy spectrum of the Hamiltonian in Eq. (6) is obtained as

$$\epsilon_s(\mathbf{k}) = t_0 k^2 + s \Delta_{\mathbf{k}}, \quad (7)$$

with $\Delta_{\mathbf{k}} = k \sqrt{\lambda^2 + t_j^2 k^2 \sin^2 2\phi}$. Both λ and t_j parameters contribute to the spin splitting ($2\Delta_{\mathbf{k}}$) between the two spin states $s = +$ and $s = -$, while t_j is responsible for the anisotropic spin splitting. The corresponding normalized eigen spinors for the spin-split dispersion are

$$|+, \mathbf{k}\rangle = \begin{bmatrix} \cos \frac{\theta_{\mathbf{k}}}{2} \\ i \sin \frac{\theta_{\mathbf{k}}}{2} e^{i\phi} \end{bmatrix}; \quad |-, \mathbf{k}\rangle = \begin{bmatrix} \sin \frac{\theta_{\mathbf{k}}}{2} \\ -i \cos \frac{\theta_{\mathbf{k}}}{2} e^{i\phi} \end{bmatrix}, \quad (8)$$

where $\theta_{\mathbf{k}} = \cos^{-1} \left[\frac{t_j k^2 \sin 2\phi}{\Delta_{\mathbf{k}}} \right]$. The spin orientation of an electron with wave vector \mathbf{k} in the Rashba coupled altermagnet system is $\langle \sigma \rangle_s = \{\langle \sigma_x \rangle_s, \langle \sigma_y \rangle_s, \langle \sigma_z \rangle_s\} = s \{-\sin \theta_{\mathbf{k}} \sin \phi, \sin \theta_{\mathbf{k}} \cos \phi, \cos \theta_{\mathbf{k}}\}$. Thus, the spin and linear momentum lock in a way such that $\langle \sigma \rangle_s \cdot \mathbf{k} = 0$. Figure (1) depicts the band structure for the Rashba coupled altermagnet systems. Unlike the Rashba spin-splitting, the spin splitting here is anisotropic. The minimum SOC splitting occurs along the azimuthal directions $\phi = n\pi/2$ (n : an integer) (where the two spin vectors are tangential to the (k_x, k_y) plane), whereas the same is maximum for $\phi = (2n + 1)\pi/4$ (where the σ_z component of the two spin vectors is maximum). Considering an excitation with energy ϵ , the wave vector in the Rashba coupled altermagnet system for band s can

be written as

$$k_s(\phi) = \left[\frac{\lambda^2 + 2t_0\epsilon + s[\lambda^4 + 4t_0\lambda^2\epsilon + (2t_j\epsilon \sin 2\phi)^2]^{\frac{1}{2}}}{2(t_0^2 - t_j^2 \sin^2 2\phi)} \right]^{\frac{1}{2}}, \quad (9)$$

and the density of states is given by

$$\rho_s(\epsilon) = \frac{1}{4\pi^2 t_0} \int_0^{2\pi} \frac{1}{\left| 2 + \frac{s[\lambda^2 + 2t_j^2 k_s(\phi)^2 \sin^2 2\phi]}{t_0 [\lambda^2 k_s(\phi)^2 + t_j^2 k_s(\phi)^4 \sin^2 2\phi]} \right|^{1/2}} d\phi. \quad (10)$$

Moreover, the Berry curvature corresponding to s band can be obtained as

$$\Omega_s(\mathbf{k}) = s \frac{\lambda^2 t_j k^2 \sin 2\phi}{2\Delta_{\mathbf{k}}^3} \hat{z}, \quad (11)$$

which exhibits anisotropic even-parity characteristic (a d -wave signature). The gap closing at the origin results in a singularity in $\Omega_s(\mathbf{k})$. In contrast, a counterpart ferromagnet-Rashba model, $t_0\sigma_0 k^2 + \lambda(\sigma_y k_x - \sigma_x k_y) + M\sigma_z$ (M is the mass gap generated by breaking the time-reversal symmetry), yields an isotropic Berry curvature near the Γ point, consistent with the fundamentally isotropic s -wave character of ferromagnetism [66]. It is important to note that the Berry curvature vanishes when either $t_j = 0$ or $\lambda = 0$. This indicates that a nonzero Berry curvature arises only from the combined breaking of inversion and PT symmetries. Now, the generalized velocity components for Rashba coupled altermagnet system arising from band velocity are given by

$$\begin{aligned} \langle \hat{v}_{b,x} \rangle &= \frac{1}{\hbar} [2t_0 k \cos \phi + 2st_j k \cos \theta_{\mathbf{k}} \sin \phi + \lambda s \sin \theta_{\mathbf{k}} \cos \phi], \\ \langle \hat{v}_{b,y} \rangle &= \frac{1}{\hbar} [2t_0 k \sin \phi + 2st_j k \cos \theta_{\mathbf{k}} \cos \phi + \lambda s \sin \theta_{\mathbf{k}} \sin \phi], \end{aligned}$$

while the velocity components arising from anomalous velocity are obtained as

$$\langle \hat{v}_{a,x} \rangle = -\frac{e}{\hbar} E_y \Omega_z, \quad \langle \hat{v}_{a,y} \rangle = \frac{e}{\hbar} E_x \Omega_z.$$

Further, the spin velocity components resulting from the band velocity are derived as follows

$$\begin{aligned} \langle \hat{v}_{b,xx} \rangle &= -\frac{1}{\hbar} st_0 k \sin \theta_{\mathbf{k}} \sin 2\phi, \\ \langle \hat{v}_{b,xy} \rangle &= \frac{1}{\hbar} [\lambda + 2st_0 k \sin \theta_{\mathbf{k}} \cos^2 \phi], \\ \langle \hat{v}_{b,xz} \rangle &= \frac{2}{\hbar} [t_j k \sin \phi + st_0 k \cos \theta_{\mathbf{k}} \cos \phi], \\ \langle \hat{v}_{b,yx} \rangle &= -\frac{1}{\hbar} [\lambda + 2st_0 k \sin \theta_{\mathbf{k}} \sin^2 \phi], \\ \langle \hat{v}_{b,yy} \rangle &= \frac{1}{\hbar} st_0 k \sin \theta_{\mathbf{k}} \sin 2\phi \\ \langle \hat{v}_{b,yz} \rangle &= \frac{2}{\hbar} [t_j k \cos \phi + st_0 k \cos \theta_{\mathbf{k}} \sin \phi]. \end{aligned}$$

It is important to note that the spin velocity resulting from band component with out-of-plane polarization ($\langle \hat{v}_{b,xz} \rangle$ and $\langle \hat{v}_{b,yz} \rangle$) vanishes in the pure Rashba case, since for $t_j = 0$, $\cos \theta_{\mathbf{k}} = 0$. We find that these components ($\langle \hat{v}_{b,xz} \rangle$ and $\langle \hat{v}_{b,yz} \rangle$) are responsible for the spin-Hall current (a transverse spin current with out-of-plane polarization) in altermagnetic system, which we discuss in detail later. Now the spin velocity components resulting from the anomalous velocity are obtained as

$$\begin{aligned} \langle \hat{v}_{a,xx} \rangle &= s \frac{e}{\hbar} E_y \Omega_z \sin \theta_{\mathbf{k}} \sin \phi, \\ \langle \hat{v}_{a,xy} \rangle &= -s \frac{e}{\hbar} E_y \Omega_z \sin \theta_{\mathbf{k}} \cos \phi, \\ \langle \hat{v}_{a,xz} \rangle &= -s \frac{e}{\hbar} E_y \Omega_z \cos \theta_{\mathbf{k}}, \\ \langle \hat{v}_{a,yx} \rangle &= -s \frac{e}{\hbar} E_x \Omega_z \sin \theta_{\mathbf{k}} \sin \phi, \\ \langle \hat{v}_{a,yy} \rangle &= s \frac{e}{\hbar} E_x \Omega_z \sin \theta_{\mathbf{k}} \cos \phi, \\ \langle \hat{v}_{a,yz} \rangle &= s \frac{e}{\hbar} E_x \Omega_z \cos \theta_{\mathbf{k}}. \end{aligned}$$

which exist only in systems with nonzero Berry curvature. Here as well, the spin velocity component with out-of-plane polarization contributes to the spin-Hall current; however, this contribution is negligible compared to that from the band component (elaborated later). In a pure altermagnetic system, the spin-Hall current arises solely from the spin velocity resulting from band component.

III. RESULTS AND DISCUSSIONS

This section presents the results for different order spin currents along with the associated discussions. The plots for spin current are presented as a function of Fermi energy (ϵ_F) for different values of t_j and λ . For all plots, we consider $t_0 = \hbar^2/(2m^*) = 0.761$ eV.nm² with $m^* = 0.05m_e$ being the effective mass (m_e : electronic mass). Further, we consider three values of altermagnet and Rashba parameter as $\lambda = 0.02, 0.04, 0.06$ eV.nm and $t_j = [0.2, 0.4, 0.6]t_0$, respectively. The temperature for all the plots is fixed at $T = 0$ K.

A. Background spin current

First we present the results for the nonpropagating background spin current [50]. Using Eq. (4) with $n = 0$, we find that $\mathcal{J}_{xx}^{(0)} = \mathcal{J}_{yy}^{(0)} = 0$. Similarly, we find $\mathcal{J}_{xz}^{(0)} = \mathcal{J}_{yz}^{(0)} = 0$. On the other hand, we obtain $\mathcal{J}_{xy}^{(0)} \neq 0$ and $\mathcal{J}_{yx}^{(0)} \neq 0$. At zero temperature $\mathcal{J}_{xy}^{(0)}$ and $\mathcal{J}_{yx}^{(0)}$ have the following forms (for details, please see Eq. (A1) in

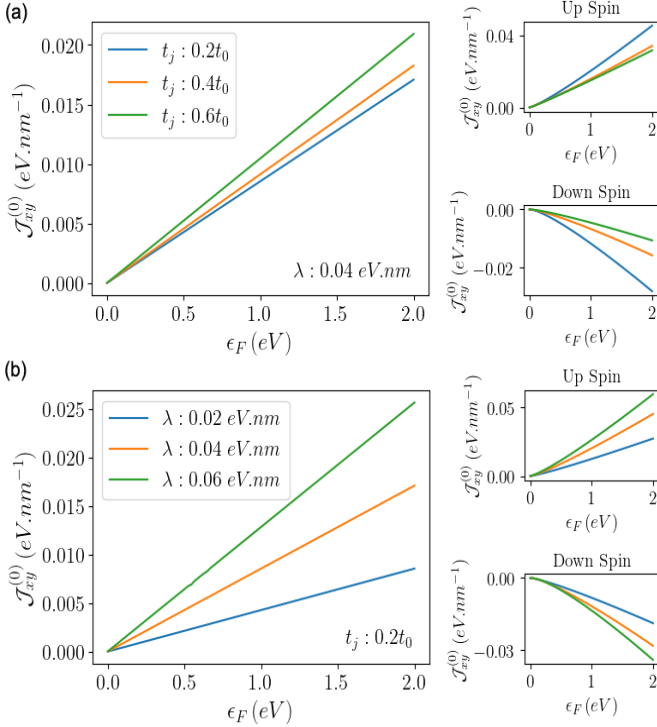


FIG. 2. The background spin current $\mathcal{J}_{xy}^{(0)}$ (in $\text{eV}\cdot\text{nm}^{-1}$) as a function of Fermi energy ϵ_F (in eV) (a) for different values of t_j with $\lambda = 0.04 \text{ eV}\cdot\text{nm}$ and (b) for different values of λ with $t_j = 0.2 t_0$. The corresponding spin-split current is shown in the right panel.

Appendix A)

$$\mathcal{J}_{xy}^{(0)} = \frac{\lambda}{16\pi^2} \sum_s \int_0^{2\pi} \left[[k_s^F(\phi)]^2 + 2st_0 \left(\frac{\Delta_s^F(\phi)}{t_j^2 \sin^2(2\phi)} \right) - \lambda^2 \frac{\tanh^{-1} \left[\frac{t_j [k_s^F(\phi)]^2 \sin(2\phi)}{\Delta_s^F(\phi)} \right]}{[t_j \sin(2\phi)]^3} \right] \cos^2 \phi d\phi,$$

$$\mathcal{J}_{yx}^{(0)} = -\frac{\lambda}{16\pi^2} \sum_s \int_0^{2\pi} \left[[k_s^F(\phi)]^2 + 2st_0 \left(\frac{\Delta_s^F(\phi)}{t_j^2 \sin^2(2\phi)} \right) - \lambda^2 \frac{\tanh^{-1} \left[\frac{t_j [k_s^F(\phi)]^2 \sin(2\phi)}{\Delta_s^F(\phi)} \right]}{[t_j \sin(2\phi)]^3} \right] \sin^2 \phi d\phi,$$

where $\Delta_s^F(\phi) = k_s^F(\phi)[\lambda^2 + t_j^2 [k_s^F(\phi)]^2 \sin^2(2\phi)]^{1/2}$ with $k_s^F(\phi)$ being the wavevector at $\epsilon = \epsilon_F$ for band s . Evaluating the ϕ integration in Eq. (12), we obtain that $\mathcal{J}_{xy}^{(0)} = -\mathcal{J}_{yx}^{(0)}$. Here, it is to be noted that for pure Rashba case ($t_j = 0$, $\lambda \neq 0$) also, one can find $\mathcal{J}_{xx}^{(0)} = \mathcal{J}_{yy}^{(0)} = \mathcal{J}_{xz}^{(0)} = \mathcal{J}_{yz}^{(0)} = 0$ and $\mathcal{J}_{xy}^{(0)} = -\mathcal{J}_{yx}^{(0)} \neq 0$ [50]. In the case of altermagnet Rashba ($t_j \neq 0$, $\lambda \neq 0$), one might expect the t_j term to contribute to $\mathcal{J}_{xz}^{(0)}$ or $\mathcal{J}_{yz}^{(0)}$, unlike the pure Rashba case ($t_j = 0$). However, this contribution is absent because the terms involving t_j

that would affect the spin current $\mathcal{J}_{xz}^{(0)}$ and $\mathcal{J}_{yz}^{(0)}$ vanish upon integration over ϕ (see the expressions for $\langle \hat{v}_{b,xz} \rangle_s$ and $\langle \hat{v}_{b,yz} \rangle_s$). Though the altermagnet term influences the behavior of the background spin current, it does not create it on its own, as $\mathcal{J}_{xy}^{(0)} = \mathcal{J}_{yx}^{(0)} = 0$ for $\lambda = 0$. Thus, the background spin current is a characteristic of the inversion-breaking system, as it vanishes when inversion symmetry is restored.

In Fig. (2), we show the plots for background spin current $\mathcal{J}_{xy}^{(0)}$ as a function of Fermi energy ϵ_F . The upper plot represents the spin current for different values of t_j with $\lambda = 0.04 \text{ eV}\cdot\text{nm}$, while the lower panel represents the spin current for different values of λ with $t_j = 0.2 t_0$. The background spin current for Rashba coupled altermagnet systems appears nearly linear as a function of Fermi energy. The right panel displays the individual spin contributions to the background spin current, clearly illustrating how the total spin current varies with Fermi energy. It is worth noting that in the pure 2D Rashba case ($t_j = 0$, $\lambda \neq 0$), the background spin current is independent of Fermi energy when $\epsilon_F > 0$ [50]. Additionally, we observe that both t_j and λ contribute to an enhancement of the background spin current.

B. Linear Spin current

Here we present the results of the linear spin current for all possible combinations. First, we consider the linear spin current arising from the band velocity (calculated from Eq. (4) with $n = 1$), where we find $\mathcal{J}_{b,xx}^{(1),x} = \mathcal{J}_{b,xx}^{(1),y} = \mathcal{J}_{b,xy}^{(1),x} = \mathcal{J}_{b,xy}^{(1),y} = \mathcal{J}_{b,xz}^{(1),x} = \mathcal{J}_{b,yx}^{(1),x} = \mathcal{J}_{b,yx}^{(1),y} = \mathcal{J}_{b,yy}^{(1),x} = \mathcal{J}_{b,yy}^{(1),y} = \mathcal{J}_{b,yz}^{(1),x} = \mathcal{J}_{b,yz}^{(1),y} = 0$ and $\mathcal{J}_{b,xz}^{(1),x} \neq 0$ and $\mathcal{J}_{b,yz}^{(1),x} \neq 0$. Therefore, linear currents arising from band velocity vanish if the propagation direction aligns with either the polarization direction or the direction of the electric field and hence the spin currents always have out-plane spin polarization. These linear spin currents transverse to the electric field with out-of-plane spin polarization ($\mathcal{J}_{b,yz}^{(1),x}$ and $\mathcal{J}_{b,xz}^{(1),y}$) can be interpreted as spin Hall currents. In the pure 2D Rashba case ($t_j = 0$, $\lambda \neq 0$, $M = 0$) [50], as well as in the gapped 2D Rashba case ($t_j = 0$, $\lambda \neq 0$, $M \neq 0$) [62], there are no linear currents originating from band velocity. In a gapped 2D Rashba system, the spin Hall current arises solely from the anomalous velocity, which is induced by a nonzero Berry curvature resulting from the breaking of both inversion and time-reversal symmetries [62]. In our system, t_j is responsible for the band-induced linear spin Hall current and hence, the altermagnetic system can be considered as a promising candidate for the generation of spin Hall current.

At zero temperature, the band induced linear spin Hall currents have the following forms (for details, please see

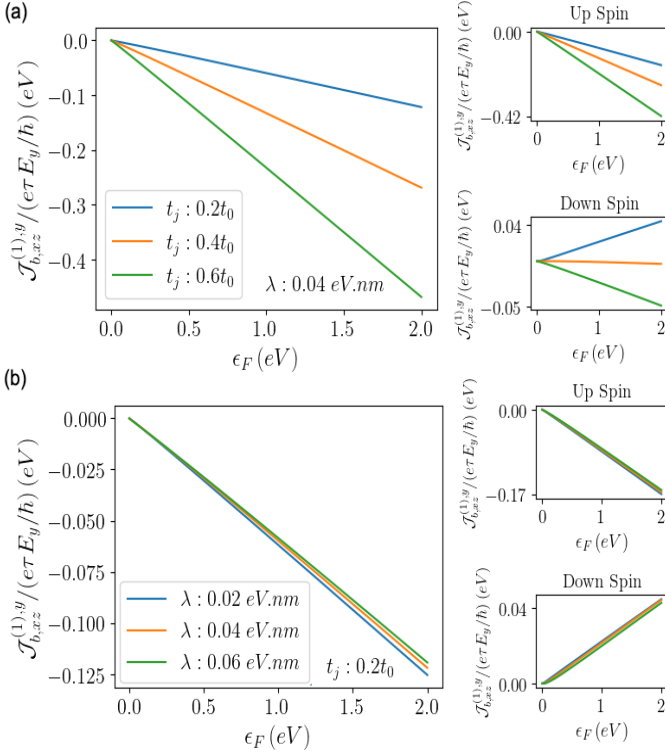


FIG. 3. The plots for $\mathcal{J}_{b,xz}^{(1),y}/(e\tau E_y/\hbar)$ (in eV), ($\mathcal{J}_{b,xz}^{(1),y}$: linear spin Hall current from band velocity) as a function of Fermi energy ϵ_F (in eV) (a) for different values of t_j with $\lambda = 0.04$ eV.nm and (b) for different values of λ with $t_j = 0.2 t_0$. The right panel displays the corresponding spin-split current.

Eq. (A2) in Appendix A)

$$\begin{aligned}
\mathcal{J}_{b,xz}^{(1),y} &= \frac{-e\tau E_y}{4\hbar\pi^2} \sum_s \int_0^{2\pi} \left[2t_0 k \sin \phi + 2st_j \right. \\
&\quad \times \left. k \cos \theta_k \cos \phi + \lambda s \sin \theta_k \sin \phi \right]_{\epsilon=\epsilon_F(\phi)} \\
&\quad \times \left[st_0 k \cos \theta_k \cos \phi + t_j k \sin \phi \right]_{\epsilon=\epsilon_F(\phi)} \\
&\quad \times \left| k \frac{\partial k}{\partial \epsilon} \right|_{\epsilon=\epsilon_F(\phi)} d\phi, \\
\mathcal{J}_{b,yz}^{(1),x} &= \frac{-e\tau E_x}{4\hbar\pi^2} \sum_s \int_0^{2\pi} \left[2t_0 k \cos \phi + 2st_j \right. \\
&\quad \times \left. k \cos \theta_k \sin \phi + \lambda s \sin \theta_k \cos \phi \right]_{\epsilon=\epsilon_F(\phi)} \\
&\quad \times \left[st_0 k \cos \theta_k \sin \phi + t_j k \cos \phi \right]_{\epsilon=\epsilon_F(\phi)} \\
&\quad \times \left| k \frac{\partial k}{\partial \epsilon} \right|_{\epsilon=\epsilon_F(\phi)} d\phi,
\end{aligned} \quad (13)$$

where we find that $\mathcal{J}_{b,xz}^{(1),y} = \mathcal{J}_{b,yz}^{(1),x}$ in case of $E_x = E_y$.

In Fig. (3), we present the plots for $\mathcal{J}_{b,xz}^{(1),y}/(e\tau E_y/\hbar)$ as a function of Fermi energy. The upper plot shows the spin current for different values of t_j with $\lambda = 0.04$ eV.nm, while the lower plot displays the spin current

for different values of λ with $t_j = 0.2 t_0$. The linear spin current originating from the band velocity increases in magnitude with the Fermi energy, displaying a linear dependence. To elucidate the contributions of different spin channels to the spin current, the spin-split current is presented in the right panel. As expected, the altermagnetic parameter (t_j) leads to an enhancement of the first-order spin current magnitude. Conversely, the Rashba parameter (λ) induces a slight suppression of the current, although its overall contribution remains comparatively weak. This is because the contributions from the spin-up and spin-down channels nearly cancel each other as λ varies.

Now, we consider the linear spin current arising from the anomalous velocity (calculated from Eq. (5) with $n = 0$), where we find that $\mathcal{J}_{a,xx}^{(1),x} = \mathcal{J}_{a,xy}^{(1),y} = \mathcal{J}_{a,xz}^{(1),z} = \mathcal{J}_{a,yx}^{(1),x} = \mathcal{J}_{a,yz}^{(1),z} = \mathcal{J}_{a,yy}^{(1),y} = \mathcal{J}_{a,yz}^{(1),y} = 0$ and $\mathcal{J}_{a,xz}^{(1),y} \neq 0$ and $\mathcal{J}_{a,yz}^{(1),x} \neq 0$. Similar to the linear spin currents arising from band velocity, the linear spin currents in this case also consistently exhibit out-of-plane spin polarization. These spin currents can also be interpreted as spin Hall currents arising from a nonzero Berry curvature, which requires both the altermagnetic parameter and the Rashba coupling to be nonzero. At zero temperature, the linear spin Hall currents arising from anomalous velocity have the following forms (for details, please see Eq. (A3) in Appendix A)

$$\begin{aligned}
\mathcal{J}_{a,xz}^{(1),y} &= \frac{eE_y\lambda^2}{32\pi^2} \sum_s \int_0^{2\pi} \left(\frac{1}{\lambda^2 + [t_j k_s^F(\phi) \sin(2\phi)]^2} \right. \\
&\quad \left. - \frac{1}{\lambda^2} \right) d\phi \\
\mathcal{J}_{a,yz}^{(1),x} &= -\frac{eE_x\lambda^2}{32\pi^2} \sum_s \int_0^{2\pi} \left(\frac{1}{\lambda^2 + [t_j k_s^F(\phi) \sin(2\phi)]^2} \right. \\
&\quad \left. - \frac{1}{\lambda^2} \right) d\phi
\end{aligned} \quad (14)$$

and hence we obtain $\mathcal{J}_{a,xz}^{(1),y} = -\mathcal{J}_{a,yz}^{(1),x}$ with the consideration $E_x = E_y$. Since we obtain $\mathcal{J}_{b,xz}^{(1),y} = \mathcal{J}_{b,yz}^{(1),x}$ and $\mathcal{J}_{a,xz}^{(1),y} = -\mathcal{J}_{a,yz}^{(1),x}$, the total spin current (considering both the band and anomalous components) $\mathcal{J}_{xz}^{(1),y}$ ($\mathcal{J}_{b,xz}^{(1),y} + \mathcal{J}_{a,xz}^{(1),y}$) and $\mathcal{J}_{yz}^{(1),x}$ ($\mathcal{J}_{b,yz}^{(1),x} + \mathcal{J}_{a,yz}^{(1),x}$) have different values (even with the consideration $E_x = E_y$). Thus, unlike the 2D gapped Rashba case [62], in the 2D altermagnet-Rashba system, the spin Hall current is driven not only by the Berry curvature but also by the band velocity inherent to the altermagnet.

In Fig. (4), we present the plot for the linear spin Hall current $\mathcal{J}_{a,xz}^{(1),y}/(eE_y)$ as a function of Fermi energy ϵ_F . As earlier, the upper plot displays the spin current for different values of t_j with $\lambda = 0.04$ eV.nm, while the lower plot shows the spin current for different values of λ with $t_j = 0.2 t_0$. The magnitude of the linear spin Hall current arising from anomalous velocity increases with Fermi energy, though its behavior differs from that of

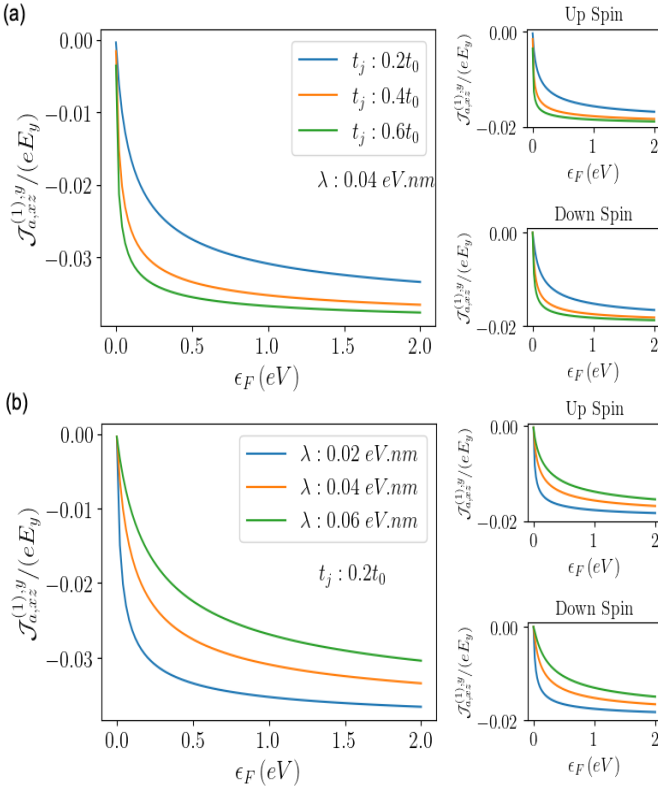


FIG. 4. The plots for $\mathcal{J}_{a,xz}^{(1),y}/(eE_y)$ (dimensionless) ($\mathcal{J}_{a,xz}^{(1),y}$: linear spin Hall current from anomalous velocity) as a function of Fermi energy ϵ_F (in eV) (a) for different values of t_j with $\lambda = 0.04$ eV.nm and (b) for different values of λ with $t_j = 0.2 t_0$. The corresponding spin-split current is shown in the right panel.

the spin Hall current induced by band velocity. At higher Fermi energies, the anomalous-velocity-induced spin Hall current tends to saturate, in contrast to the band-induced spin Hall current, which continues to grow. As before, t_j enhances the magnitude of the linear spin Hall current induced by anomalous velocity; however, increasing the Rashba strength leads to the opposite effect.

Next, we compare the linear spin Hall currents induced by band velocity and anomalous velocity with $\tau = 2.5$ ps. As shown in Fig. (5), $\mathcal{J}_{b,xz}^{(1),y}/(eE_y)$ is significantly larger than $\mathcal{J}_{a,xz}^{(1),y}/(eE_y)$. This indicates that, although the Berry curvature contributes to the spin Hall current, the band velocity plays the dominant role in realizing spin Hall currents in Rashba-coupled altermagnets. Moreover, in a pure altermagnetic system, the spin Hall current arises entirely from the band velocity, as the Berry curvature vanishes when $\lambda = 0$.

C. Nonlinear spin current

In the previous subsection, we showed that the transverse linear spin current is finite, while the longitudinal

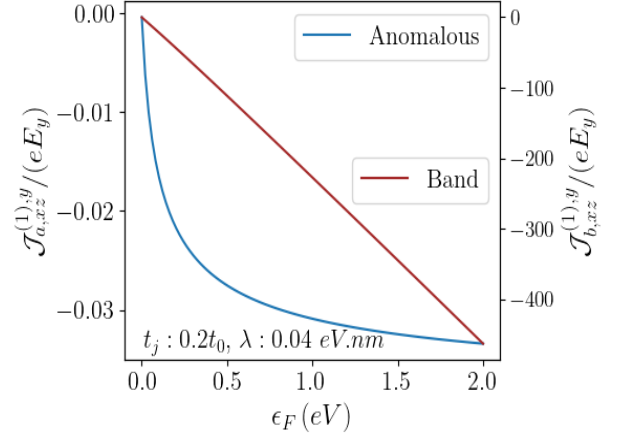


FIG. 5. The plots for $\mathcal{J}_{b,xz}^{(1),y}/(eE_y)$ (dimensionless) and $\mathcal{J}_{a,xz}^{(1),y}/(eE_y)$ (dimensionless) as a function of Fermi energy ϵ_F (in eV) with $\tau = 2.5$ ps. This confirms that the band velocity plays the dominant role in realizing spin Hall currents in Rashba-coupled altermagnets.

component vanishes. The leading nonzero contribution to the longitudinal spin current is quadratic in the electric field \mathbf{E} , a hallmark of systems with broken inversion symmetry. In this subsection, we analyze the quadratic spin current under different configurations of spin orientation, charge transport direction, and applied electric field. We begin by presenting cases where the quadratic spin current arises purely from the band velocity. At zero temperature, the expression for the non-linear current arising from the band velocity takes the following form (for details, please see Eq. (A5) in Appendix A)

$$\mathcal{J}_{b,ij}^{(2),\eta} = \frac{\hbar e^2 \tau^2 E_\eta^2}{16\pi^2} \sum_s \int_0^{2\pi} \left[\frac{\partial}{\partial \epsilon} [\mathcal{H}_s(\epsilon)] \right]_{\epsilon = \epsilon_F(\phi)} d\phi \quad (15)$$

with $\mathcal{H}_s(\epsilon) = |k \frac{\partial k}{\partial \epsilon} \langle \hat{v}_{b,ij} \rangle_s \langle \hat{v}_{b,\eta} \rangle_s^2$.

Results for $\mathcal{J}_{b,xx}^{(2),\eta}$, $\mathcal{J}_{b,yy}^{(2),\eta}$: Now we shall present results for quadratic spin currents, $\mathcal{J}_{b,xx}^{(2),\eta}$ and $\mathcal{J}_{b,yy}^{(2),\eta}$ when both propagation and polarization are in the same direction. Here we find $\mathcal{J}_{b,xx}^{(2),x} = \mathcal{J}_{b,xx}^{(2),y} = \mathcal{J}_{b,yy}^{(2),x} = \mathcal{J}_{b,yy}^{(2),y} = 0$. Thus, the band velocity does not contribute to the non-linear spin currents when the propagation and polarization directions are the same. The same phenomenon was also observed in the 2D gapped Rashba system [62].

Results for $\mathcal{J}_{b,xy}^{(2),\eta}$, $\mathcal{J}_{b,yx}^{(2),\eta}$: Here we present the results for quadratic spin currents $\mathcal{J}_{b,xy}^{(2),\eta}$, $\mathcal{J}_{b,yx}^{(2),\eta}$, where we consider the in-plane polarization, but the propagation and polarization direction are perpendicular to each other. Interestingly, we find $\mathcal{J}_{b,xy}^{(2),x} = -\mathcal{J}_{b,yx}^{(2),y} \neq 0$ and $\mathcal{J}_{b,xy}^{(2),y} = -\mathcal{J}_{b,yx}^{(2),x} \neq 0$. Therefore, the band velocity contributes to both the longitudinal and transverse non linear spin currents. In Figs. (6) and (7), we present the plots for $\mathcal{J}_{b,xy}^{(2),x}/(e\tau E_x/4\pi\hbar)^2$ and $\mathcal{J}_{b,xy}^{(2),y}/(e\tau E_y/4\pi\hbar)^2$ as a function of Fermi energy ϵ_F . As earlier cases, the upper

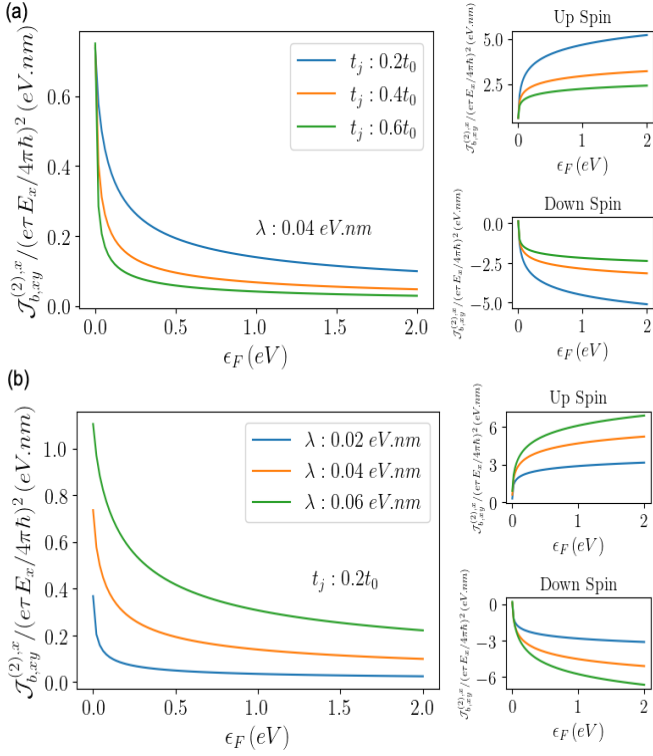


FIG. 6. The plots for $\mathcal{J}_{b,xy}^{(2),x}/(\epsilon\tau E_x/4\pi\hbar)^2$ (in eV.nm) ($\mathcal{J}_{b,xy}^{(2),x}$: nonlinear longitudinal spin current from band velocity) as a function of Fermi energy ϵ_F (in eV) (a) for different values of t_j with $\lambda = 0.04$ eV.nm and (b) for different values of λ with $t_j = 0.2 t_0$. The right panel displays the corresponding spin-split current.

plots show the spin current for different values of t_j with $\lambda = 0.04$ eV.nm, while the lower plots display the spin current for different values of λ with $t_j = 0.2 t_0$. To clarify the individual contributions of distinct spin channels to the overall spin current, the corresponding spin-split current is depicted in the right panel. For longitudinal current, the nonlinear spin current originating from band velocity reaches its maximum at lower Fermi energy values, then decreases as the Fermi energy increases, eventually saturating at higher Fermi energies. Furthermore, the altermagnetic term reduces the longitudinal nonlinear current, while the Rashba term enhances it. However, the transverse nonlinear spin current originating from band velocity exhibits a different behavior as a function of Fermi energy. It shows an increasing trend with Fermi energy and eventually saturates at higher Fermi energies. Furthermore, the nonlinear transverse spin current from band velocity exhibits a nonmonotonic dependence on the altermagnet parameter, whereas the Rashba spin-orbit coupling consistently enhances the transverse spin current.

Results for $\mathcal{J}_{b,xz}^{(2),\eta}$, $\mathcal{J}_{b,yz}^{(2),\eta}$. Now, we consider the case where the polarization is out of the plane. Here, we obtain that $\mathcal{J}_{b,xz}^{(2),\eta} = \mathcal{J}_{b,yz}^{(2),\eta} = 0$. It should be noted that although the t_j term contributes to spin velocity oper-

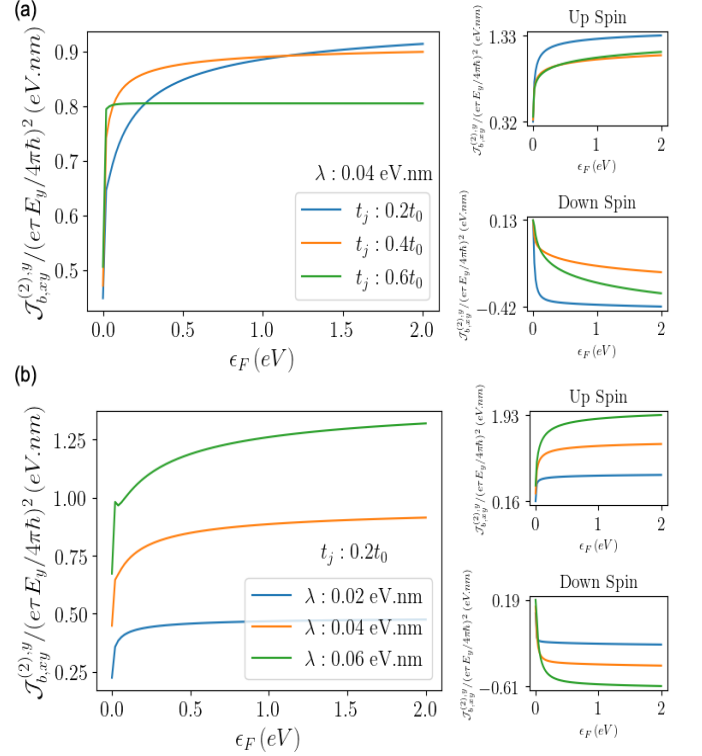


FIG. 7. The plots for $\mathcal{J}_{b,xy}^{(2),y}/(\epsilon\tau E_y/4\pi\hbar)^2$ (in eV.nm) ($\mathcal{J}_{b,xy}^{(2),y}$: nonlinear transverse spin current from band velocity) as a function of Fermi energy ϵ_F (in eV) (a) for different values of t_j with $\lambda = 0.04$ eV.nm and (b) for different values of λ with $t_j = 0.2 t_0$. The corresponding spin-split current is shown in the right panel.

ators $\langle \hat{v}_{b,xz} \rangle_s$ and $\langle \hat{v}_{b,yz} \rangle_s$ (unlike the pure 2D Rashba case), it does not contribute to $\mathcal{J}_{b,xz}^{(2),\eta}$ and $\mathcal{J}_{b,yz}^{(2),\eta}$ due to the ϕ integration. Thus, the spin currents with out-of-plane polarization due to band velocity are always of linear order in the electric field.

Now, we consider the nonlinear spin current arising from the anomalous velocity. At zero temperature, the expression for the nonlinear spin current due to anomalous velocity takes the following form (for details, please see Eq. (A6) in Appendix A)

$$\mathcal{J}_{a,ij}^{(2),\eta} = -\frac{\hbar\epsilon\tau E_\eta}{8\pi^2} \sum_s \int_0^{2\pi} \left[\left| k \frac{\partial k}{\partial \epsilon} \right| \langle \hat{v}_{a,ij} \rangle_s \times \langle \hat{v}_{b,\eta} \rangle_s \right]_{\epsilon=\epsilon_F(\phi)} d\phi. \quad (16)$$

Results for $\mathcal{J}_{a,xx}^{(2),y}$, $\mathcal{J}_{a,xy}^{(2),y}$, $\mathcal{J}_{a,yx}^{(2),x}$, $\mathcal{J}_{a,yy}^{(2),x}$. Here we consider the nonlinear transverse spin current arising from anomalous velocity with in-plane polarization where we find that $\mathcal{J}_{a,xx}^{(2),y} = \mathcal{J}_{a,yy}^{(2),x} = 0$ and $\mathcal{J}_{a,xy}^{(2),y} = \mathcal{J}_{a,yx}^{(2),x} \neq 0$ with the consideration $E_x = E_y$. Here it should be noted that for gapped 2D Rashba case [62], the scenario is opposite, where $\mathcal{J}_{a,xx}^{(2),y} = \mathcal{J}_{a,yy}^{(2),x} \neq 0$ and $\mathcal{J}_{a,xy}^{(2),y} = \mathcal{J}_{a,yx}^{(2),x} = 0$. For the 2D gapped Rashba case, the mass gap M (which

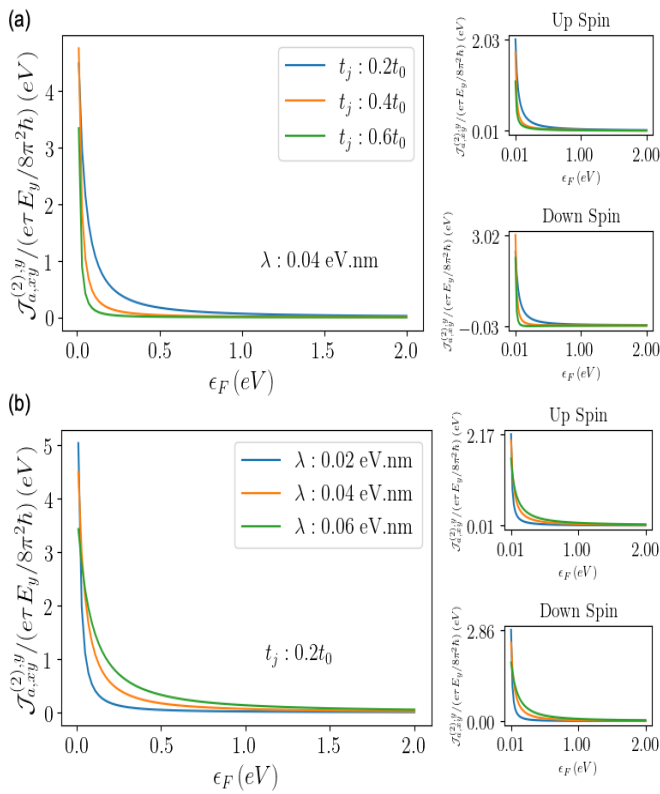


FIG. 8. The plots for $\mathcal{J}_{a,xy}^{(2),y}/(e\tau E_y/8\pi^2\hbar)$ (in eV) ($\mathcal{J}_{a,xy}^{(2),y}$: nonlinear transverse spin current from anomalous velocity) as a function of Fermi energy ϵ_F (in eV) (a) for different values of t_j with $\lambda = 0.04$ eV.nm and (b) for different values of λ with $t_j = 0.2 t_0$. The right panel displays the corresponding spin-split current.

is absent in our case) is responsible for $\mathcal{J}_{a,xx}^{(2),y} = \mathcal{J}_{a,yy}^{(2),x} \neq 0$, whereas in our case, the altermagnet t_j term is responsible for $\mathcal{J}_{a,xy}^{(2),y} = \mathcal{J}_{a,yx}^{(2),x} \neq 0$ (which is absent in 2D gapped Rashba case). In Fig. (8), we present the plot for nonlinear spin current $\mathcal{J}_{a,xy}^{(2),y}/(e\tau E_y/8\pi^2\hbar)$ as a function of Fermi energy ϵ_F . The plots show that as ϵ_F approaches 0, the nonlinear spin current arising from anomalous velocity peaks, then begins to decrease, and eventually becomes zero at higher Fermi energies. Furthermore, t_j reduces the nonlinear spin current originating from anomalous velocity, whereas the Rashba term enhances it.

Results for $\mathcal{J}_{a,xz}^{(2),y}, \mathcal{J}_{a,yz}^{(2),x}$: Here we consider the nonlinear transverse spin current arising from anomalous velocity with out of plane polarization, where we find that $\mathcal{J}_{a,xz}^{(2),y} = \mathcal{J}_{a,yz}^{(2),x} = 0$. Thus, the spin current with out-of-plane polarization is always linear with respect to the electric field. The nonlinear transverse spin currents consist of both band and anomalous components. For instance, at $\tau = 2.5$ ps and $E_y = 10^3$ V/m, the Berry curvature contribution dominates over the band contribution—opposite to what is observed in the linear spin Hall current. All the above results of spin current (whether it

Spin current	$\mathbf{E} = 0$	$\eta = x$ (B)	$\eta = x$ (A)	$\eta = y$ (B)	$\eta = y$ (A)
$\mathcal{J}_{xx}^{(0)}$	0	NA	NA	NA	NA
$\mathcal{J}_{xy}^{(0)}$	Finite	NA	NA	NA	NA
$\mathcal{J}_{xz}^{(0)}$	0	NA	NA	NA	NA
$\mathcal{J}_{xx}^{1,\eta}$	NA	0	0	0	0
$\mathcal{J}_{xy}^{1,\eta}$	NA	0	0	0	0
$\mathcal{J}_{xz}^{1,\eta}$	NA	0	0	Finite	Finite
$\mathcal{J}_{xx}^{2,\eta}$	NA	0	0	0	0
$\mathcal{J}_{xy}^{2,\eta}$	NA	Finite	0	Finite	Finite
$\mathcal{J}_{xz}^{2,\eta}$	NA	0	0	0	0

*NA: Not Applicable, *B: Band component contribution, *A: Anomalous component contribution

TABLE I. Nature of spin currents in 2D Rashba coupled altermagnet system for different orientations of electric field \mathbf{E} .

is zero or non-zero) are tabulated in Table I.

IV. CONCLUSION

We have investigated the background, linear, and nonlinear spin currents in 2D Rashba spin-orbit coupled altermagnet systems, considering their distinct contributions to spin current generation. It is well established that the Rashba term breaks inversion symmetry, while the altermagnet term breaks combined parity (P) and time-reversal (T) symmetry (PT symmetry) and these broken symmetries play a crucial role in shaping spin current behavior. Our analysis incorporates Berry curvature-induced anomalous velocity corrections within the semiclassical equations of motion, which give rise to transverse linear and nonlinear spin currents. The study primarily focuses on the interplay between the altermagnet parameter (t_j) and the Rashba parameter (λ) in relation to spin currents as a function of Fermi energy (ϵ_F).

We find that the background spin current emerges solely in the presence of spin-orbit coupling, with the altermagnet term (t_j) significantly influencing its behavior but unable to generate it independently. It consistently exhibits in-plane polarization, with the propagation direction perpendicular to this polarization. The background spin current increases nearly linearly with Fermi energy and is enhanced by both the altermagnet and Rashba parameters.

The most interesting finding of our study is the band velocity induced linear spin Hall current—absent in a simple Rashba-coupled system ($t_j = 0$)—underscoring its potential as a promising source of spin Hall current generation. Linear spin currents are always transverse with out-of-plane polarization and can be interpreted as Spin Hall currents arising from both band and anomalous velocities, with band velocity playing the primary role in their realization in Rashba-coupled altermagnets. It is important to note that the anomalous component of the

spin Hall current vanishes at $\lambda = 0$, whereas the band-induced spin Hall current remains nonzero. The magnitude of the band-driven linear spin Hall current increases almost linearly with Fermi energy, while the magnitude of anomalous velocity contribution initially rises but saturates at higher energies. Additionally, the altermagnet parameter enhances the absolute value of linear spin Hall current, whereas the Rashba parameter suppresses it.

The leading nonzero longitudinal spin current is quadratic in the electric field \mathbf{E} , a signature of broken inversion symmetry. Unlike linear spin currents, nonlinear spin currents feature both longitudinal and transverse components with in-plane polarization, where the propagation direction is perpendicular to the polarization. The longitudinal component from band velocity decreases and saturates with increasing ϵ_F , while the transverse component grows before saturating. In contrast, the transverse contribution from anomalous velocity diminishes with ϵ_F and almost vanishes at high ϵ_F . The altermagnet pa-

rameter t_j suppresses the nonlinear longitudinal current, while the Rashba parameter λ enhances it. The transverse current from band velocity is enhanced by λ and shows a non-monotonic dependence on t_j , whereas t_j reduces and λ increases the transverse current from anomalous velocity. The nonlinear transverse spin current with in-plane polarization comprises both band velocity and anomalous velocity contributions, with the anomalous contribution being the dominant component. This comprehensive study of the interplay between Rashba and altermagnet parameters may provide valuable insights for controlling spin currents in Rashba spin-orbit coupled altermagnet systems.

V. ACKNOWLEDGEMENT

Author acknowledges Prof. T. K. Ghosh for useful discussions.

Appendix A: Detail calculation of spin currents

At zero temperature the background spin current $\mathcal{J}_{xy}^{(0)}$ can be calculated as follows

$$\begin{aligned}
\mathcal{J}_{xy}^{(0)} &= \frac{\hbar}{2} \frac{1}{(2\pi)^2} \sum_s \int d^2k \langle \hat{v}_{b,xy} \rangle_s \\
&= \frac{1}{2} \frac{1}{(2\pi)^2} \sum_s \int \int [\lambda + 2st_0 k \sin \theta_k \cos^2 \phi] k dk d\phi \\
&= \frac{1}{2} \frac{1}{(2\pi)^2} \sum_s \left[\lambda \int \left(\int k dk \right) d\phi + 2st_0 \int \left(\int k^2 \sin \theta_k dk \right) \cos^2 \phi d\phi \right] \\
&= \frac{1}{2} \frac{1}{(2\pi)^2} \sum_s \left[\lambda \int_0^{2\pi} \left(\int_0^{k_s^F(\phi)} k dk \right) d\phi + 2s\lambda t_0 \int_0^{2\pi} \left(\int_0^{k_s^F(\phi)} \frac{k^2}{\sqrt{\lambda^2 + t_j^2 k^2 \sin^2(2\phi)}} dk \right) \cos^2 \phi d\phi \right] \\
&= \frac{\lambda}{16\pi^2} \sum_s \int_0^{2\pi} \left[[k_s^F(\phi)]^2 + 2st_0 \left(\frac{\Delta_s^F(\phi)}{t_j^2 \sin^2(2\phi)} - \lambda^2 \frac{\tanh^{-1} \left[\frac{t_j [k_s^F(\phi)]^2 \sin(2\phi)}{\Delta_s^F(\phi)} \right]}{[t_j \sin(2\phi)]^3} \right) \right] \cos^2 \phi d\phi.
\end{aligned} \tag{A1}$$

At zero temperature the linear spin Hall current $\mathcal{J}_{b,xz}^{(1),y}$ arising from band velocity can be calculated as follows

$$\begin{aligned}
\mathcal{J}_{b,xz}^{(1),y} &= \frac{\hbar}{2} \frac{1}{(2\pi)^2} \sum_s \int d^2k \langle \hat{v}_{b,xz} \rangle f_1 \\
&= \frac{e\tau E_y \hbar}{8\pi^2} \sum_s \int d^2k \langle \hat{v}_{b,xz} \rangle \langle \hat{v}_{b,y} \rangle \frac{\partial f_0}{\partial \epsilon} \\
&= - \frac{e\tau E_y}{4\pi^2 \hbar} \sum_s \int \int |k \frac{\partial k}{\partial \epsilon}| [st_0 k \cos \theta_k \cos \phi + t_j k \sin \phi] [2t_0 k \sin \phi + 2st_j k \cos \theta_k \cos \phi + \lambda s \sin \theta_k \sin \phi] \delta(\epsilon - \epsilon_F) d\epsilon d\phi \\
&= \frac{-e\tau E_y}{4\hbar\pi^2} \sum_s \int_0^{2\pi} \left[[st_0 k \cos \theta_k \cos \phi + t_j k \sin \phi] [2t_0 k \sin \phi + 2st_j k \cos \theta_k \cos \phi + \lambda s \sin \theta_k \sin \phi] \left| k \frac{\partial k}{\partial \epsilon} \right| \right]_{\epsilon = \epsilon_F(\phi)} d\phi.
\end{aligned} \tag{A2}$$

At zero temperature the linear spin Hall current $\mathcal{J}_{a,xz}^{(1),y}$ arising from anomalous velocity can be calculated as follows

$$\begin{aligned}
\mathcal{J}_{a,xz}^{(1),y} &= \frac{\hbar}{2} \frac{1}{(2\pi)^2} \sum_s \int d^2k \langle \hat{v}_{a,xz} \rangle_s \\
&= - \frac{\hbar}{2} \frac{1}{(2\pi)^2} \sum_s \int \int [s \frac{e}{\hbar} E_y \Omega_z \cos \theta_k] k dk d\phi \\
&= - \frac{e E_y \lambda^2 t_j^2}{4} \frac{1}{(2\pi)^2} \sum_s \int_0^{2\pi} \left(\int_0^{k_s^F(\phi)} \frac{k}{(\lambda^2 + t_j^2 k^2 \sin^2(2\phi))^2} dk \right) \sin(2\phi)^2 d\phi \\
&= \frac{e E_y \lambda^2}{32\pi^2} \sum_s \int_0^{2\pi} \left(\frac{1}{\lambda^2 + [t_j k_s^F(\phi) \sin(2\phi)]^2} - \frac{1}{\lambda^2} \right) d\phi.
\end{aligned} \tag{A3}$$

At zero temperature the non linear spin current $\mathcal{J}_{b,ij}^{(2),\eta}$ arising from band velocity can be calculated as follows

$$\begin{aligned}
\mathcal{J}_{b,ij}^{(2),\eta} &= \frac{\hbar}{2} \frac{1}{(2\pi)^2} \sum_s \int d^2k \langle \hat{v}_{b,ij} \rangle_s f_2 \\
&= \frac{\hbar (e\tau E_\eta)^2}{16\pi^2} \sum_s \int \int |k \frac{\partial k}{\partial \epsilon}| \langle \hat{v}_{b,ij} \rangle_s \langle v_{b,\eta} \rangle_s^2 \frac{\partial^2 f_0}{\partial \epsilon^2} d\epsilon d\phi \\
&= \frac{\hbar (e\tau E_\eta)^2}{16\pi^2} \sum_s \int \int \mathcal{H}_s(k(\epsilon)) \frac{\partial^2 f_0}{\partial \epsilon^2} d\epsilon d\phi
\end{aligned} \tag{A4}$$

Performing integration by parts with $\mathcal{H}_s(k(\epsilon)) = |k \frac{\partial k}{\partial \epsilon}| \langle \hat{v}_{b,ij} \rangle_s \langle v_{b,\eta} \rangle_s^2$, we have

$$\begin{aligned}
\mathcal{J}_{b,ij}^{(2),\eta} &= - \frac{\hbar (e\tau E_\eta)^2}{16\pi^2} \sum_s \int \int \left[\frac{\partial}{\partial \epsilon} \mathcal{H}_s(k(\epsilon)) \frac{\partial f_0}{\partial \epsilon} \right] d\epsilon d\phi \\
&= \frac{\hbar (e\tau E_\eta)^2}{16\pi^2} \sum_s \int \left[\frac{\partial}{\partial \epsilon} [\mathcal{H}_s(k(\epsilon))] \right]_{\epsilon=\epsilon_F(\phi)} d\phi.
\end{aligned} \tag{A5}$$

At zero temperature the non linear spin current $\mathcal{J}_{a,ij}^{(2),\eta}$ arising from anomalous velocity can be calculated as follows

$$\begin{aligned}
\mathcal{J}_{a,ij}^{(2),\eta} &= \frac{\hbar}{2} \frac{1}{(2\pi)^2} \sum_s \int d^2k \langle \hat{v}_{a,ij} \rangle_s f_1 \\
&= \frac{\hbar e\tau E_\eta}{8\pi^2} \sum_s \int \int \left[|k \frac{\partial k}{\partial \epsilon}| \langle \hat{v}_{a,ij} \rangle_s \langle v_{b,\eta} \rangle_s \frac{\partial f_0}{\partial \epsilon} \right] d\epsilon d\phi \\
&= - \frac{\hbar e\tau E_\eta}{8\pi^2} \sum_s \int \left[|k \frac{\partial k}{\partial \epsilon}| \langle \hat{v}_{a,ij} \rangle_s \langle v_{b,\eta} \rangle_s \right]_{\epsilon=\epsilon_F(\phi)} d\phi.
\end{aligned} \tag{A6}$$

-
- [1] I. Mazin and The PRX Editors, Phys. Rev. X **12**, 040002 (2022).
[2] L. Smejkal, A. B. Hellenes, R. G. Hernandez, J. Sinova, and T. Jungwirth, Phys. Rev. X **12**, 011028 (2022).
[3] H.-Y. Ma, M. Hu, N. Li, J. Liu, W. Yao, J.-F. Jia, and J. Liu, Nat. Commun. **12**, 2846 (2021).
[4] R. G. Hernandez, L. Smejkal, K. Vyborny, Y. Yahagi, J. Sinova, T. Jungwirth, and J. Zelezny, Phys. Rev. Lett. **126**, 127701 (2021).
[5] A. Bose, N. J. Schreiber, R. Jain, D.-F. Shao, H. P. Nair,

- J. Sun, X. S. Zhang, D. A. Muller, E. Y. Tsympal, D. G. Schlom, and D. C. Ralph, Nat. Electron. **5**, 267 (2022).
[6] H. Bai, L. Han, X. Y. Feng, Y. J. Zhou, R. X. Su, Q. Wang, L. Y. Liao, W. X. Zhu, X. Z. Chen, F. Pan, X. L. Fan, and C. Song, Phys. Rev. Lett. **128**, 197202 (2022).
[7] S. Karube, T. Tanaka, D. Sugawara, N. Kadoguchi, M. Kohda, and J. Nitta, Phys. Rev. Lett. **129**, 137201 (2022).
[8] D.-F. Shao, S.-H. Zhang, M. Li, C.-B. Eom, and E. Tsympal, Nat. Commun. **12**, 7061 (2021).

- [9] L. Smejkal, A. H. MacDonald, J. Sinova, S. Nakatsuji, and T. Jungwirth, *Nat. Rev. Mater.* **7**, 482 (2022).
- [10] Z. Feng, X. Zhou, L. Smejkal, L. Wu, Z. Zhu, H. Guo, R. G. Hernandez, X. Wang, H. Yan, P. Qin, X. Zhang, H. Wu, H. Chen, Z. Meng, L. Liu, Z. Xia, J. Sinova, T. Jungwirth, and Z. Liu, *Nat. Electron.* **5**, **735** (2022).
- [11] R. D. G. Betancourt, J. Zubac, R. Gonzalez-Hernandez, K. Geishendorf, Z. Soban, G. Springholz, K. Olejnik, L. Smejkal, J. Sinova, T. Jungwirth, S. T. B. Goennenwein, A. Thomas, H. Reichlova, J. Zelezny, and D. Kriegner, *Phys. Rev. Lett.* **130**, 036702 (2023).
- [12] X.-Y. Hou, H.-C. Yang, Z.-X. Liu, P.-J. Guo, and Z.-Y. Lu, *Phys. Rev. B* **107**, L161109 (2023).
- [13] X. Zhou, W. Feng, X. Yang, G.-Y. Guo, and Y. Yao, *Phys. Rev. B* **104**, 024401 (2021).
- [14] X. Zhou, W. Feng, R.-W. Zhang, L. Smejkal, J. Sinova, Y. Mokrousov, and Y. Yao, *Phys. Rev. Lett.* **132**, 056701 (2024).
- [15] Y.-X. Li, Y. Liu, and C.-C. Liu, *Phys. Rev. B* **109**, L201109 (2024).
- [16] P.-J. Guo, Y. Gu, Z.-F. Gao, and Z.-Y. Lu, arXiv:2312.13911 [cond-mat.mtrl-sci] (2023).
- [17] D. Zhu, Z.-Y. Zhuang, Z. Wu, and Z. Yan, *Phys. Rev. B* **108**(2023).
- [18] Y.-X. Li and C.-C. Liu, *Phys. Rev. B* **108**, 205410 (2023).
- [19] P.-J. Guo, Z.-X. Liu, and Z.-Y. Lu, *npj Comput. Mater.* **9**, 70 (2023).
- [20] S. Qu, Z.-F. Gao, H. Sun, K. Liu, P.-J. Guo, and Z.-Y. Lu, arXiv:2401.11065 [cond-mat.mtrl-sci] (2024).
- [21] Z.-F. Gao, S. Qu, B. Zeng, Y. Liu, J.-R. Wen, H. Sun, P.-J. Guo, and Z.-Y. Lu, arXiv:2311.04418 [condmat.mes-hall] (2023).
- [22] Z. Xiao, J. Zhao, Y. Li, R. Shindou, and Z.-D. Song, *Phys. Rev. X* **14**, 031037 (2024).
- [23] S. Zeng and Y.-J. Zhao, *Phys. Rev. B* **110**, 054406 (2024).
- [24] Y. Liu, J. Yu, and C.-C. Liu, *Phys. Rev. Lett.* **133**, 206702 (2024).
- [25] O. Fedchenko, J. Minar, A. Akashdeep, S. W. D'Souza, D. Vasilyev, O. Tkach, L. Odenbreit, Q. Nguyen, D. Kutnyakhov, N. Wind, L. Wenthaus, M. Scholz, K. Rossnagel, M. Hoesch, M. Aeschlimann, B. Stadtmuller, M. Klaui, G. Schonhense, T. Jungwirth, A. B. Hellenes, G. Jakob, L. Smejkal, J. Sinova, and H. J. Elmers, *Sci. Adv.* **10**, eadj4883 (2024).
- [26] J. Krempasky, L. Smejkal, S. W. D'Souza, M. Hajlaoui, G. Springholz, K. Uhlirova, F. Alarab, P. C. Constantinou, V. Strocov, D. Usanov, W. R. Pudelko, R. G. Hernandez, A. B. Hellenes, Z. Jansa, H. Reichlova, Z. Soban, R. D. G. Betancourt, P. Wadley, J. Sinova, D. Kriegner, J. Minar, J. H. Dil, and T. Jungwirth, *Nature* **626**, 517 (2024).
- [27] T. Osumi, S. Souma, T. Aoyama, K. Yamauchi, A. Honma, K. Nakayama, T. Takahashi, K. Ohgushi, and T. Sato, *Phys. Rev. B* **109**, 115102 (2024).
- [28] L.-D. Yuan, Z. Wang, J.-W. Luo, E. I. Rashba, and A. Zunger, *Phys. Rev. B* **102**, 014422 (2020).
- [29] Q. Cui, Y. Zhu, X. Yao, P. Cui, and H. Yang, *Phys. Rev. B* **108**, 024410 (2023).
- [30] J. Sodequist and T. Olsen, *Appl. Phys. Lett.* **124**, 182409 (2024).
- [31] I. Mazin, R. G. Hernandez, and L. Smejkal, arXiv preprint arXiv:2309.02355 (2023).
- [32] S. A. Wolf, D. D. Awschalom, R. A. Buhrman, J. M. Daughton, S. von Molnar, M. L. Roukes, A. Y. Chtchelkanova, and D. M. Treger, *Science* **294**, 1488 (2001).
- [33] I. Zutic, J. Fabian, and S. Das Sarma, *Rev. Mod. Phys.* **76**, 323 (2004).
- [34] S. D. Bader and S. S. P. Parkin, *Annu. Rev. Condens. Matter Phys.* **1**, 71 (2010).
- [35] J. Schliemann, *Rev. Mod. Phys.* **89**, 011001 (2017).
- [36] S. Datta and B. Das, *App. Phys. Lett.* **56**, 665 (1990).
- [37] S. Gardelis, C. G. Smith, C. H. W. Barnes, E. H. Linfield, and D. A. Ritchie, *Phys. Rev. B* **60**, 7764 (1999).
- [38] G. Schmidt, D. Ferrand, L. W. Molenkamp, A. T. Filip, and B. J. van Wees, *Phys. Rev. B* **62**, R4790(R) (2000).
- [39] C. M. Hu, J. Nitta, A. Jensen, J. B. Hansen, and H. Takayanagi, *Phys. Rev. B* **63**, 125333 (2001).
- [40] N. Tombros, C. Jozsa, M. Popinciuc, H. T. Jonkman, and B. J. V. Wees, *Nature (London)* **448**, 571 (2007).
- [41] J. Xiao, G. E. W. Bauer, K.-C. Uchida, E. Saitoh, and S. Maekawa, *Phys. Rev. B* **81**, 214418 (2010).
- [42] S. D. Ganichev, E. L. Ivchenko, V. V. Bel'kov, S. A. Tarasenko, M. Sollinger, D. Weiss, W. Wegscheider, and W. Prettl, *Nature (London)* **417**, 153 (2002).
- [43] M. J. Stevens, A. L. Smirl, R. D. R. Bhat, A. Najmaie, J. E. Sipe, and H. M. van Driel, *Phys. Rev. Lett.* **90**, 136603 (2003).
- [44] E. I. Rashba, *Fiz. Tverd. Tela* **2**, 1224 (1960) [*Sov. Phys. Solid State* **2**, 1109 (1960)].
- [45] Y. A. Bychkov and E. I. Rashba, *J. Phys. C* **17**, 6039 (1984).
- [46] J. Nitta, T. Akazaki, H. Takayanagi, and T. Enoki, *Phys. Rev. Lett.* **78**, 1335 (1997).
- [47] G. Engels, J. Lange, T. Schapers, and H. Luth, *Phys. Rev. B* **55**, R1958 (1997).
- [48] L. Smejkal, J. Sinova, and T. Jungwirth, *Phys. Rev. X* **12**, 040501 (2022).
- [49] K. Hamamoto, M. Ezawa, K. W. Kim, T. Morimoto, and N. Nagaosa, *Phys. Rev. B* **95**, 224430 (2017).
- [50] E. I. Rashba, *Phys. Rev. B* **68**, 241315(R) (2003).
- [51] E. I. Rashba, *Phys. Rev. B* **70**, 161201(R) (2004).
- [52] D. Loss, P. Goldbart, and A. V. Balatsky, *Phys. Rev. Lett.* **65**, 1655 (1990).
- [53] J. Splettstoesser, M. Governale, and U. Zülicke, *Phys. Rev. B* **68**, 165341 (2003).
- [54] F. Schutz, M. Kollar, and P. Kopietz, *Phys. Rev. Lett.* **91**, 017205 (2003).
- [55] Usaj and C. A. Balseiro, *Europhys. Lett.* **72**, 631 (2005).
- [56] F. Dolcini and F. Rossi, *Phys. Rev. B* **98**, 045436 (2018).
- [57] L. Rossi, F. Dolcini, and F. Rossi, *Phys. Rev. B* **101**, 195421 (2020).
- [58] Y. K. Kato, R. C. Myers, A. C. Gossard, and D. D. Awschalom, *Science* **306**, 1910 (2004).
- [59] C. Day, *Phys. Today* **58**(2), 17 (2005).
- [60] H. Yu, Y. Wu, G.-B. Liu, X. Xu, and W. Yao, *Phys. Rev. Lett.* **113**, 156603 (2014).
- [61] A. Pan and D. C. Marinescu, *Phys. Rev. B* **99**, 245204 (2019).
- [62] P. Kapri, B. Dey and T. K. Ghosh *Phys. Rev. B* **103**, 165401 (2021).
- [63] M.-C Chang and Qian Niu, *Phys. Rev. Lett.* **75**, 1348 (1995).
- [64] G. Sundaram and Q. Niu, *Phys. Rev. B* **59**, 14915 (1999).
- [65] I. Sodemann and L. Fu, *Phys. Rev. Lett.* **115**, 216806 (2015).
- [66] N. Nagaosa, J. Sinova, S. Onoda, A. H. MacDonald, and N. P. Ong, *Rev. Mod. Phys.* **82**, 1539 (2010).